



Perturbing pro-survival proteins using quinoxaline derivatives: A structure–activity relationship study

Rajkumar Rajule^{a,†}, Vashti C. Bryant^{a,†}, Hernando Lopez^{a,†}, Xu Luo^a, Amarnath Natarajan^{a,b,*}

^a Eppley Institute for Cancer Research, University of Nebraska Medical Center, Omaha, NE 68198, United States

^b Department of Pharmaceutical Sciences, University of Nebraska Medical Center, Omaha, NE 68198, United States

ARTICLE INFO

Article history:

Received 8 December 2011

Revised 30 January 2012

Accepted 7 February 2012

Available online 16 February 2012

Keywords:

Quinoxaline

Structure–activity relationship

Mcl-1

Bcl-xL

ABT-737

ABSTRACT

In HeLa cells the combinatorial knockdown of Bcl-xL and Mcl-1 is sufficient to induce spontaneous apoptosis. Quinoxaline derivatives were screened for the induction of Mcl-1 dependent apoptosis using a cell line without functional Bcl-xL. Quinoxaline urea analog **1h** was able to specifically induce apoptosis in an Mcl-1 dependent manner. We demonstrate that even small changes to **1h** results in dramatic loss of activity. In addition, **1h** and ABT-737 synergistically inhibit cell growth and induce apoptosis. Our results also suggest that **1h** could have therapeutic potential against ABT-737 refractory cancer.

© 2012 Elsevier Ltd. All rights reserved.

1. Introduction

Benzopyrazine or commonly known as quinoxaline is a naphthalene isostere with carbon atoms 1 and 4 replaced with nitrogen atoms. Quinoxalines are an important class of heterocycles found in natural products. Examples include the cyclic peptide triostin A and the recently isolated Izumiphenazines A–C (Fig. 1).¹ The quinoxaline core is also found in several drugs currently on the market. They include brimonidine used to treat glaucoma, quina-cillin that has anti-bacterial properties and the smoking cessation agent varenicline (Fig. 1).² Several quinoxaline analogs are in pre-clinical and clinical development against a variety of diseases. Kinase inhibitors BMS345541 and NVP-BSK805 are being explored as an anti-tumor agent and to treat polycythemia, respectively.³ R(+)-XK469 is an example of a quinoxaline analog in clinics to treat patients with advanced refractory solid tumors (Fig. 1).⁴ Additionally compounds containing the quinoxaline core were identified as hits from recent high throughput screening campaigns.⁵ We identified a quinoxaline urea analog (NCGC55879-01) as a BRCA1 inhibitor from a quantitative high throughput screen.⁶ These

studies show that the quinoxaline analogs act as ligands for a variety of biological targets and have activities against several diseases, which fit definition of a privileged scaffold.^{1a} This led to the synthesis of focused libraries of quinoxaline analogs to further explore the chemical space and structure–activity relationship studies.⁷

An intricate network of protein–protein interactions between pro-apoptotic and pro-survival family proteins maintains a balance between cell survival and cell death.⁸ There are three types of apoptotic proteins, the anti-apoptotic (Bcl-xL, Bcl-2, Bcl-2 and Mcl-1), the initial pro-apoptotic proteins (Bad, Bim, Puma and Noxa) and cell death proteins (Bak and Bax). The pro-apoptotic proteins Bax and Bak undergo oligomerization upon activation by apoptotic stimuli.⁹ This triggers permeabilization of the mitochondrial membrane, release of apoptotic factors such as cytochrome c,¹⁰ activation of effector caspases and cell death.¹¹ The sequestration of pro-apoptotic proteins by the pro-survival Bcl-2 family proteins suppresses mitochondrial damage and ensures cell survival.¹² Increased levels of pro-survival proteins (Bcl-2, Bcl-xL or Mcl-1) are associated with maintenance of malignant diseases, resistance to chemotherapy and poor clinical outcome.¹³ These observations triggered a concerted effort to identify small molecule inhibitors and develop strategies to perturb the levels of pro-survival Bcl-2 family of proteins.

The most successful Bcl-2 inhibitors discovered to date are the ABT series of compounds from the Abbott laboratories. The crystal structure of Bcl-xL–BH3 peptide complex revealed the presence of a hydrophobic core formed by the BH1-3 domains of Bcl-xL that binds a α -helix peptide found in BH3 only proteins.¹⁴ A structure

Abbreviations: Mcl-1, myeloid cell leukemia 1; Bcl-xL, B-cell lymphoma extra large; Bcl-2, B-cell lymphoma 2; BH, Bcl-2 homology; XIAP, X-linked inhibitor of apoptosis protein; PARP, poly (ADP-ribose) polymerase; Dox, doxycycline; GFP, green fluorescent protein.

* Corresponding author. Tel.: +1 402 559 3793; fax: +1 402 559 8270.

E-mail address: anatarajan@unmc.edu (A. Natarajan).

[†] These authors contributed equally to this work.

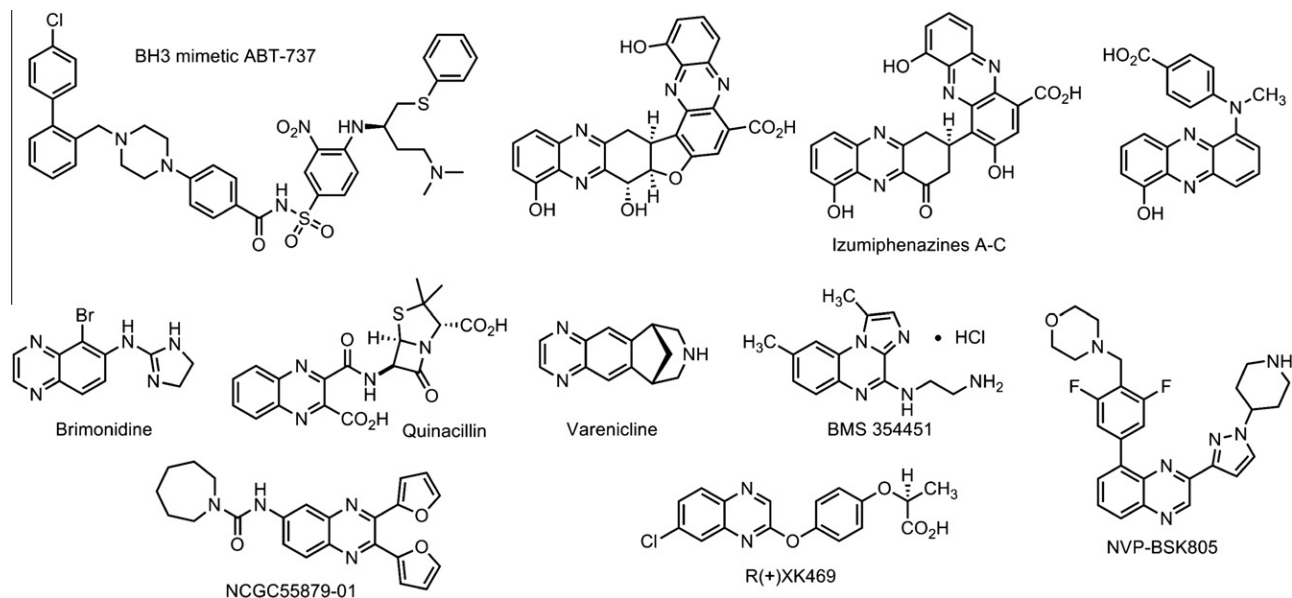


Figure 1. The BH3 mimetic ABT-737 and quinoxaline core containing natural products, drugs on the market, preclinical agents, a clinical compound and a hit from a high throughput screen.

guided fragment based design led to the development of ABT-737 a small molecule BH3 mimetic.¹⁵ ABT-737 had nanomolar binding affinities for Bcl-xL and Bcl-2 but did not bind Mcl-1.¹⁶ In vitro preclinical studies showed that ABT-737 induced apoptosis in multiple cancer cell lines at micromolar concentrations.¹⁷ Interestingly, down regulation of Mcl-1 resulted in sensitization to ABT-737 both in vitro and in vivo.¹⁸

A combination of knockdown and biochemical studies on the entire collection of prosurvival protein and BH3 only proteins were conducted to understand their roles in apoptosis.¹⁹ These studies revealed that knock down of Mcl-1 or Bcl-xL did not induce apoptosis however the combinatorial knockdown of Mcl-1 and Bcl-xL resulted in spontaneous apoptosis (without an external stimulus).²⁰ These are consistent with the sensitization of cells to ABT-737 upon Mcl-1 knock down. They also highlight the emerging functional importance of Mcl-1 and the need to develop inhibitors that perturb Mcl-1 levels.²¹

A major challenge in directly targeting Mcl-1 is the complexity associated with its regulation. Mcl-1 levels and its functions are regulated rapidly through changes in transcription, a number of posttranslational modifications that affect its localization, its stability and its ability to form a variety of protein–protein interactions (Fig. 2).²² On the other hand the various proteins that regulate Mcl-1 levels are attractive targets for inhibitor development.²¹ In the present study, we screened a focused quinoxaline library using a cell line without functional Bcl-xL, Bcl-2 and Bcl-w (accomplished by the inducible expression of the BH3 only protein Bad3SA). We identified a quinoxaline urea analog **1h** as a Mcl-1 pathway inhibitor. Mechanism specific inhibition by **1h** was established using cell lines in which levels of functional Mcl-1 and Bcl-xL was regulated by the inducible expression of BH3 only proteins Noxa and Bad3SA, respectively. Structure–activity relationship revealed the functional groups on **1h** required for activity. Follow-up studies showed that **1h** reduced Mcl-1 levels in a dose- and time-dependent manner. Compound **1h** also sensitized cells to ABT-737 and the combination of **1h** and ABT-737 resulted in rapid cleavage of Poly (ADP-Ribose) Polymerase (PARP) a biochemical marker of apoptosis. We are currently working on establishing the molecular target of **1h**, which will be reported in due course.

2. Results and discussion

2.1. Quinoxaline analogs screened for Mcl-1 depended apoptosis

Recent reports have shown that quinoxaline analogs have growth inhibitory and apoptotic activity against several cancer cell lines.^{23,7b} The quinoxaline analogs **1a–1o** screened here for anti-Mcl-1 activity were previously reported by us to have anti-proliferative activity.^{7b} The emergence of Mcl-1 as a potential target led us to screen quinoxaline analogs for Mcl-1 specific inhibitors. We used a cell line (Dox-Bad3SA) that expressed Bad3SA (a BH3 only protein that binds Bcl-xL) under doxycycline control. In the presence of doxycycline the Dox-Bad3SA cell line will express Bad3SA, which will bind and inactivate Bcl-xL leaving functional Mcl-1 to control cell survival.^{19,20} Therefore compounds that are Mcl-1 pathway specific inhibitors will show enhanced apoptosis in Dox-Bad3SA cells only in the presence of doxycycline. For this screen Dox-Bad3SA cells were incubated for 6 h with the inhibitors (10 μ M) in the presence and absence of doxycycline. Induction of apoptosis was measured using caspase 3/7 activity assay (normalized for cell number using alamarBlue).²⁴ Camptothecin (50 μ M) and a Bayer IKK β inhibitor IKK2VII (10 μ M)²⁵ a compound with a well characterized target were used as controls in this screen. Camptothecin increases the stability of Noxa protein which, competes with the Mcl-1–Bak complex to release free bak and thereby induce apoptosis.^{25c}

The quinoxaline library is described in Table 1. The results from the screen are summarized as a bar chart in Figure 3. The black bars represent caspase activity in Dox-Bad3SA HeLa cells (–Dox) with functional Bcl-xL and Mcl-1 while the grey bars represent the same with only functional Mcl-1 (+Dox). As expected, camptothecin shows increased caspase 3/7 activity in the cells with only functional Mcl-1 when compared to cells with function Bcl-xL and Mcl-1. On the other hand IKK2VII shows the opposite effect. Quinoxaline analogs **1d**, **1f**, **1j**, **1l** and **1n** show little to no effect on Dox-Bad3SA both in the presence or absence of doxycycline and are therefore classified as inactive. Compounds **1a**, **1c**, **1g**, and **1m** show increased caspase activity in Dox-Bad3SA cells both

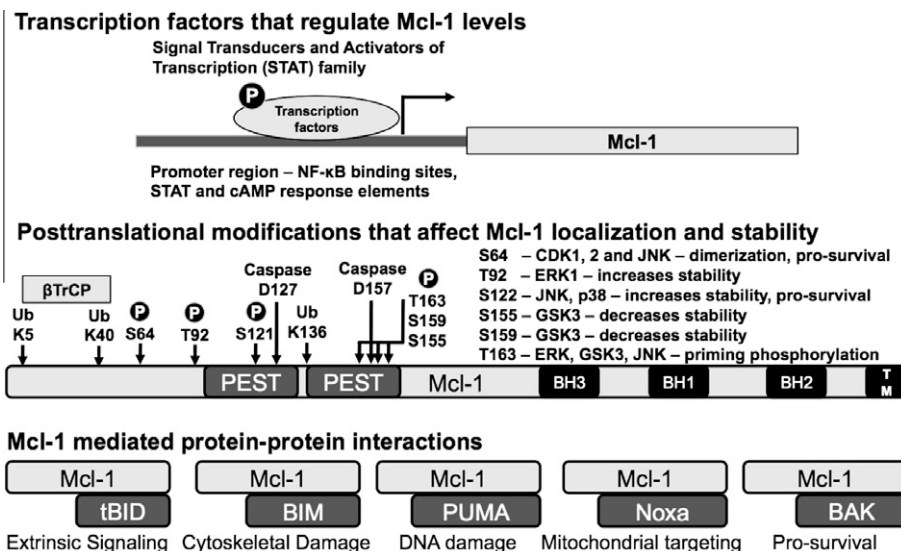


Figure 2. An overview of the modes of regulation of Mcl-1 function.

Table 1
Focused library of quinoxaline analogs

Entry	R ¹	X	R ²
1a	Methyl	O	–CH ₃
1b	Methyl	O	–NH-phenyl
1c	Methyl	O	–NH-(4-benzyl)-piperidine
1d	2-Furanyl	O	–CH ₃
1e	2-Furanyl	O	–NH-phenyl
1f	2-Furanyl	S	–NH-phenyl
1g	2-Furanyl	O	–NH-(4-fluoro)-Ph
1h	2-Furanyl	O	–NH-(4-bromo)-Ph
1i	2-Furanyl	O	–NH-4-biphenyl
1j	2-Furanyl	S	–NH-(4-nitro)-Ph
1k	2-Furanyl	O	–N-Pyrrolidine
1l	2-Furanyl	O	–N-Morpholine
1m	2-Furanyl	O	–NH-(4-benzyl)-piperidine
1n	Phenyl	S	–NH-(4-nitro)-Ph
1o	Phenyl	O	–N-Pyrrolidine

in the presence and absence of doxycycline and are therefore classified as non-specific inhibitors. Compounds **1b**, **1e** and **1i** are trending to be IKK2VII like suggesting that they have Mcl-1 agonist like function. Compounds **1h**, **1k** and **1o** show the desired Mcl-1 dependent caspase activation. It is interesting to note that going from –H to –F to –Br in **1e** to **1g** to **1h**, respectively resulted in a systematic trending towards Mcl-1 dependent caspase activation. Also, a comparison of caspase activation by compounds **1k** and **1o** suggests the need to explore the R¹ position. Therefore, we decided to generate a second set of quinoxaline analogs to explore analog **1h** further.

2.2. Synthesis and evaluation of quinoxaline urea 1h analogs

To explore the functional groups at the R¹ position and the positional effect of the bromine atom in **1h** we generated a second set of quinoxaline analogs. The quinoxaline core was generated by condensation of symmetrical diones **2a–e** with 4-nitrobenzene-1,2-diamine (**3**). Reduction of the resulting nitro compounds

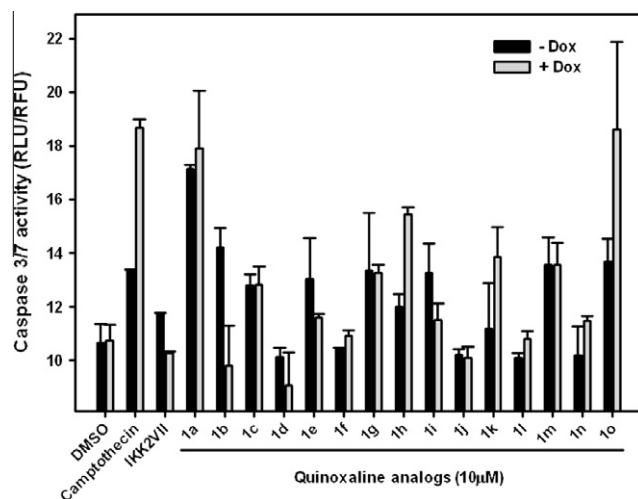
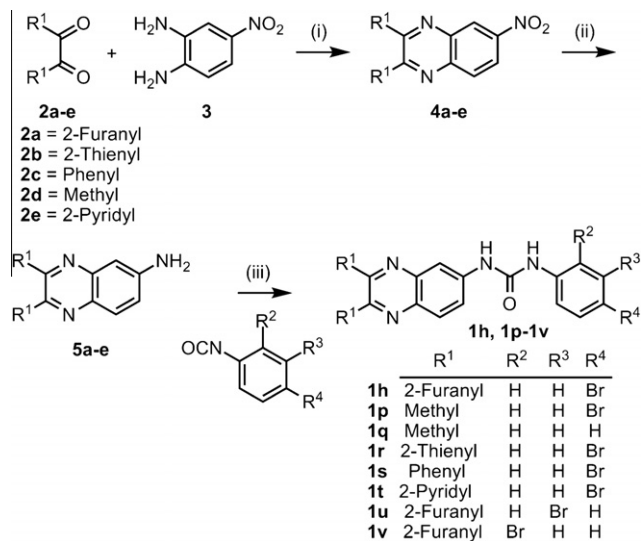


Figure 3. Induction of Mcl-1 dependent apoptosis by quinoxaline analogs. Dox-Bad3SA cells were treated with indicated compounds in the absence (–Dox) and presence (+Dox) of doxycycline. Caspase activity was measured 6 h after treatment.

4a–e to the amine **5a–e** followed by condensation with substituted isocyanates yielded the quinoxaline urea analogs **1p–v** (Scheme 1).^{7b}

The compounds were screened as described in the previous section. Except cell death was quantified after a 12 h incubation by Hoechst staining. The results from this screen are summarized in Figure 4. Replacing the furanyl rings at the R¹ position with methyl groups in analog **1p** resulted in a complete loss of activity. Not surprisingly removal of both the bromine atom at R⁴ and furanyl rings at R¹ in analog **1q** also resulted in a complete loss of activity. Replacing the oxygen atoms in the furanyl rings with sulfur atoms in analog **1r** resulted in a significant (>90%) loss of activity. On the other hand, replacing the furanyl rings with phenyl rings in analog **1s** resulted in retention of activity. Interestingly replacing the phenyl rings with pyridyl rings in analog **1t** also resulted in a complete loss of activity. A comparison of the activities of **1h**, **1r**, **1s** and **1t** suggests that a chelation driven conformational change could be responsible for the loss of activity in **1r** and **1t**. We next probed the positional effects of the bromine atom in compounds **1u** (*meta*)



Scheme 1. Synthesis of **1h** analogs. Reagents and conditions: (i) Ethanol, reflux (85–99%); (ii) H₂/Pd-C, ethanol, 25–28 °C (85–96%); (iii) CH₂Cl₂, 25–28 °C (62–83%).

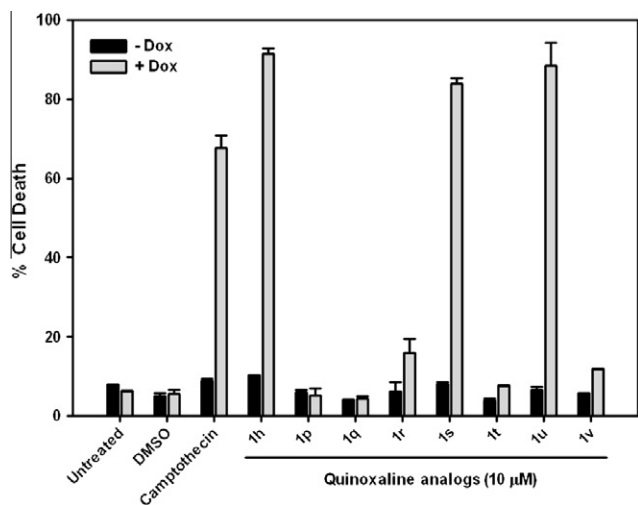


Figure 4. Structure-activity relationship with quinoxaline analogs (**1p–1v**). Dox-Bad3SA cells were treated with indicated compounds in the absence (–Dox) and presence (+Dox) of doxycycline. Cell death was measured 12 h after treatment by Hoechst staining. (See Fig. S1 for images).

and **1v** (*ortho*). Moving the bromine atom to the *meta* position in analog **1u** did not alter the activity however moving it to the *ortho* position in analog **1v** resulted in >90% loss of activity. This suggests that the –NH group in the urea could be involved in possible hydrogen bonding interactions with the molecular target of **1h**.

2.3. Follow-up studies to establish Mcl-1 dependent induction of apoptosis by analog **1h**

To demonstrate Mcl-1 dependent induction of apoptosis by **1h** we used two additional cell lines (Dox-GFP and Dox-Noxa).^{19,20} Figure 5 summarizes the functional prosurvival proteins present in these inducible cell lines. The Dox-GFP control cell line expresses GFP when treated with doxycycline and has functional Bcl-xL and Mcl-1. The Dox-Noxa cell line expresses Noxa when treated with doxycycline, which sequesters Mcl-1 and therefore has only functional Bcl-xL. The Dox-Bad3SA cell line expresses Bad3SA and has only functional Mcl-1.

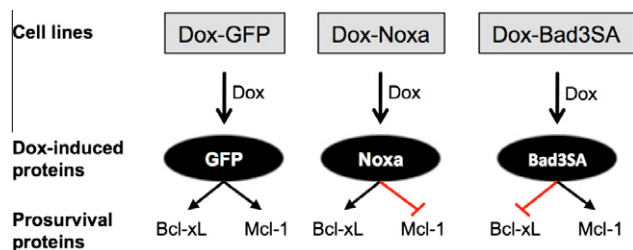


Figure 5. Doxycycline inducible cell lines used to identify Mcl-1 specific modulators. Doxycycline (Dox) treatment of cells leads to the induction of GFP, Noxa and Bad3SA expression.

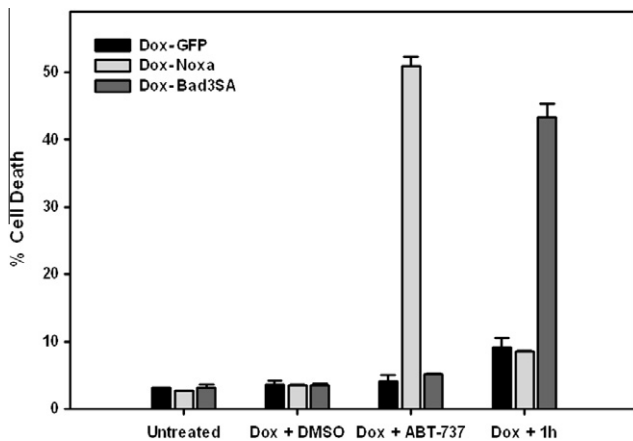


Figure 6. Compound **1h** induces cell death in a Mcl-1 specific manner. Doxycycline inducible cell lines were treated as indicated for 12 h and stained with Hoechst dye to quantify number of dead cells. (See Fig. S2 for images).

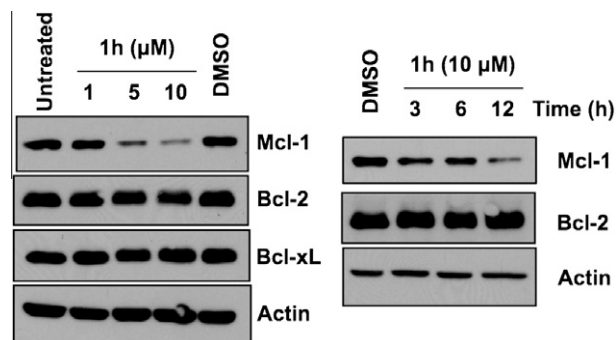


Figure 7. Down regulation of Mcl-1 by **1h**. (left) HeLa cells were incubated with the indicated concentrations of compound **1h** for 12 h. (right) HeLa cells that over-express Bcl-xL were treated with compound **1h** (10 μM) for the indicated time points. Cells were then harvested and lysates were resolved on SDS-PAGE gels. DMSO was used as a vehicle control. Actin was used as loading control.

The three cell lines, Dox-GFP, Dox-Noxa and Dox-Bad3SA were treated with doxycycline (1 μg/mL) for 3 h to induce the expression of GFP, Noxa and Bad3SA, respectively. The cells were then treated with DMSO, ABT-737 (1 μM) or **1h** (10 μM) for an additional 12 h. Under the assay conditions neither ABT-737 nor **1h** induced cell death in Dox-GFP cells. This is because ABT-737 inhibits only Bcl-xL allowing functional Mcl-1 to prevent cell death and **1h** inhibits only Mcl-1 allowing functional Bcl-xL to prevent cell death. As expected, ABT-737 induced cell death in Dox-Noxa cells, but not in Dox-Bad3SA cells. This is consistent with results reported in the literature about the specificity of ABT-737 for Bcl-2/Bcl-xL and not Mcl-1.¹⁵ Compound **1h** induced cell death only

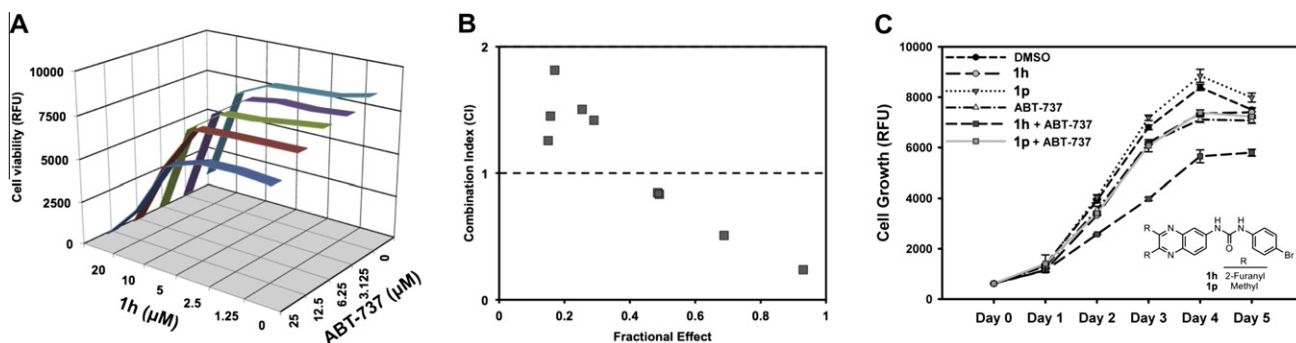


Figure 8. Synergism studies with **1h** and ABT-737. (A) Matrix of combination treatment with **1h** and ABT-737 in a cell growth assay. (B) Combination index (CI) determination using matrix data. (C) Time dependent HeLa cell growth at CI = 0.84 concentrations.

in Dox-Bad3SA cells, but not in Dox-Noxa cells demonstrating its specificity for Mcl-1 dependent apoptosis (Fig. 6).

To determine if analog **1h** perturbs Mcl-1 levels we conducted dose response (1, 5 and 10 μM of **1h** with a 12 h incubation) and time course (3, 6 and 12 h incubation at 10 μM of **1h**) studies. The lysates were subjected to SDS-PAGE and probed for prosurvival proteins (Mcl-1, Bcl-xL and Bcl-2) by Western blot analyses. We observed a dose- and time-dependent decrease of Mcl-1 levels in cells treated with **1h** (Fig. 7). For the time dependent studies we observed varying amounts of cell death in HeLa cells therefore we used HeLa cells that over express Bcl-xL.

2.4. Synergism studies with **1h** and ABT-737

Since **1h** selectively perturbs Mcl-1 levels in cells we hypothesized that **1h** and ABT-737 will synergistically inhibit growth and induce apoptosis. To test this hypothesis, we treated HeLa cells with various concentration combinations of **1h** and ABT-737 and monitored cell growth (Fig. 8A). Data from this study was used to determine combination indices (CI) for **1h** and ABT-737 (Fig. 8B).²⁶ CI < 1 indicates synergy; CI \sim 1 indicates additive effects while CI > 1 indicates antagonism.²⁶ CI values ranging from 0.24 to 0.84 were obtained when micromolar concentrations of both drugs were used, however at lower concentrations CI values >1 were

observed. At the present time we do not fully understand the observed CI > 1. The growth inhibitory effects of the compounds ABT-737 (12.5 μM) and **1h** (10 μM) were monitored individually and in combination (CI = 0.84) over a five-day period (Fig. 8C). An inactive compound **1p** was used as a control in this experiment. The results showed a synergistic inhibition of cell growth only with the combination of **1h** and ABT-737.

We next explored if the synergistic growth inhibition extends to the induction of apoptosis by **1h** and ABT-737. Activation of caspases is considered one of the hallmarks of apoptosis. The executioner caspases cleave multiple structural and repair proteins resulting in programmed cell death.²⁷ HeLa cells were treated with either DMSO, **1h**, **1p**, ABT-737, **1h** + ABT-737 or **1p** + ABT-737 and caspase 3/7 activity was measured after a six hour incubation (Fig. 9 see inset). The compounds individually had very little effect on the induction of caspases, however the combination of **1h** and ABT-737 resulted in \sim 4-fold increase in caspase activity. No such effect was observed with the **1p** and ABT-737 combination. We also measured cell death by Hoechst staining and found a dose-dependent increase of cell death with the combination of **1h** and ABT-737 (Fig. 9). In summary we observed a synergistic induction of apoptosis with **1h** and ABT-737.

To further explore the role of **1h** in the induction of Mcl-1 dependent apoptosis and the observed synergism with ABT-737, we determined expression levels of apoptotic proteins. Activation of caspases leads to the cleavage of specific proteins such as PARP, a nuclear protein involved in DNA repair. PARP is one of the earliest proteins targeted for cleavage by caspases.²⁸ X-linked inhibitor of apoptosis protein (XIAP) binds directly to caspase-3 and blocks access to the substrates.²⁹ Peptides derived from XIAP also bind to the catalytic site of caspase-7, thereby inactivating its enzymatic function.³⁰ Therefore, we probed PARP and XIAP levels in cells treated with DMSO, ABT-737, **1h**, **1h** + ABT-737, **1p**, **1p** + ABT-737

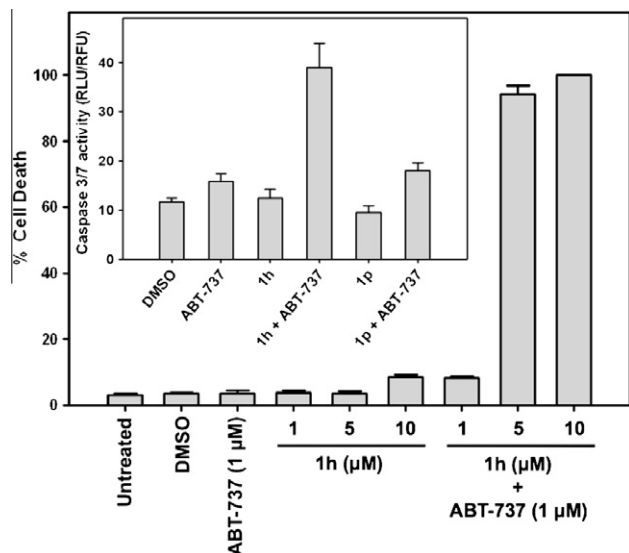


Figure 9. Apoptosis studies with **1h** and ABT-737. HeLa cells were treated as indicated and cell death was measured by Hoechst staining or caspase activity assay (inset). For the caspase assay 1 μM of ABT-737 and 10 μM of **1h** and **1p** were used. (See Fig. S3 for images).

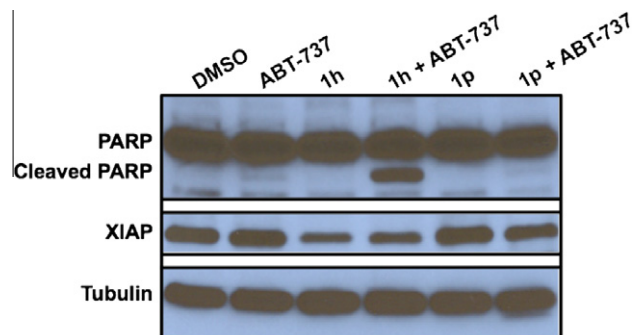


Figure 10. PARP cleavage by **1h** and ABT-737 and down regulation of XIAP in HeLa cells by **1h** evaluated by Western blotting. Tubulin was used as a loading control.

by Western blot analysis (Fig. 10). PARP cleavage was seen only in the combination of **1h** and ABT-737 and we observed reduced XIAP levels only in **1h** treated cells. This suggests that inhibiting Bcl-xL does not have any effect on XIAP levels and **1h** could be perturbing an upstream target that regulates both Mcl-1 and XIAP. Together these studies show synergistic effects of **1h** and ABT-737 in inducing apoptosis in these cells.

2.5. Conclusion

In this report, we screened a small quinoxaline library for Mcl-1 dependent apoptosis. We identified compound **1h** that had activities comparable to the positive control camptothecin which was used at fivefold higher concentrations. We generated a second set of compounds and identified the key functional groups on **1h** required for its activity. We found that small changes to **1h** resulted in significant loss of activity. Using doxycycline responsive cell lines that express GFP, Noxa and Bad3SA, we established mechanism specificity of compound **1h**. HeLa cells treated with **1h** showed a dose- and time-dependent decrease in Mcl-1 levels. We also showed that **1h** and ABT-737 synergistically inhibited cell growth and induced apoptosis. Reduction of XIAP levels in cells treated with **1h** is consistent with activation of caspases and rapid cleavage of PARP. In summary, we report the identification and characterization of quinoxaline urea analog **1h** that could have therapeutic value against ABT-737 refractory cancers.

3. Experimental methods

3.1. Chemistry general methods

All reagents were purchased from commercial sources and were used without further purification. Flash chromatography was carried out on silica gel (200–400 mesh). Thin layer chromatography (TLC) were run on pre-coated EMD silica gel 60F254 plates and observed under UV light. ¹H NMR (500 MHz) and ¹³C NMR (125 MHz) spectra were recorded in chloroform-*d* or DMSO-*d*₆ on a Varian-500 spectrometer. LC-MS for the compounds were generated on an Agilent 1200 series system with UV detector (214 nm and 254 nm) and an Agilent 6130 quadrupole mass detector. All the compounds tested were >97% pure as determined by LC. Columns and conditions used to determine purity of the compounds reported are summarized below.

Solvent A: Acetonitrile with 0.01% TFA; Solvent B: Water with 0.01% TFA. Flow rate: 1 mL/min.

Column-condition A: Agilent Zorbax 300SB_C18, narrow bore, 2.1 × 150 mm, 5 μm. 15 min gradient: 2–95% of A.

Column-condition B: Agilent Zorbax Eclipse PAH rapid resolution, 4.6 × 150 mm, 3.5 μm. 10 min gradient: 5–95% of A.

The spectral characterization data for compounds **1a–1o** and **1q** can be found in the [Supplementary Data of Ref. 7b](#).

3.2. General procedure of quinoxalinyurea derivatives 6a–i

To a stirring solution of **5a–e** (1.0 mmol) in dichloromethane (20–30 ml) under nitrogen the corresponding phenylisocyanate (1.2–1.3 mmol) was added. The mixture was maintained at room temperature for 12–48 h and the reaction monitored for completion by TLC. The precipitated solid was filtered, dried and purified by flash column chromatography to yield the desired compounds.

3.2.1. 1-(4-Bromophenyl)-3-(2,3-dimethylquinoxalin-6-yl)urea **1p**

¹H NMR (DMSO-*d*₆, 500 MHz) δ: 2.61 (s, 3H), 2.63 (s, 3H), 7.46 (s, 4H), 7.67 (dd, *J*₁ = 2.44 Hz, *J*₂ = 8.78 Hz, 1H), 7.85 (d, *J* = 8.78 Hz,

1H), 8.13 (d, *J* = 2.44 Hz, 1H), 8.98 (s, 1H), 9.15 (s, 1H). ¹³C NMR (DMSO-*d*₆, 125 MHz) δ: 23.1, 23.5, 114.1, 114.2, 120.9, 121.0, 122.5, 129.1, 132.2, 132.3, 137.3, 139.6, 140.4, 142.0, 152.2, 153.0, 154.7 MS Calcd C₁₇H₁₅BrN₄O, 370.0; Found ESI-MS *m/z*: 371.0 (M+1). Retention times, A: 6.9 min and B: 9.3 min.

3.2.2. 1-(4-Bromophenyl)-3-(2,3-di-(thiophen-2-yl)quinoxalin-6-yl)urea **1r**

¹H NMR (DMSO-*d*₆, 500 MHz) δ: 7.10 (dd, *J*₁ = 4.88 Hz, *J*₂ = 8.78 Hz, 2H), 7.16 (d, *J* = 2.93 Hz, 1H), 7.19 (d, *J* = 3.41 Hz, 1H), 7.48 (bs, 4H), 7.75 (m, 3H), 7.96 (d, *J* = 8.78 Hz, 1H), 8.28 (d, *J* = 2.44 Hz, 1H), 9.08 (s, 1H), 9.34 (s, 1H). ¹³C NMR (DMSO-*d*₆, 125 MHz) δ: 113.4, 114.4, 120.9, 121.1, 124.6, 128.4, 128.5, 129.5, 129.6, 129.8, 130.5, 132.2, 132.3, 136.8, 139.4, 139.6, 141.6, 141.7, 141.9, 142.2, 144.4, 147.0, 152.9. MS Calcd C₂₃H₁₅BrN₄OS₂, 506.0; Found ESI-MS *m/z*: 507.0 (M+1). Retention times, A: 10.7 min and B: 11.4 min.

3.2.3. 1-(4-Bromophenyl)-3-(2,3-diphenylquinoxalin-6-yl)urea **1s**

¹H NMR (DMSO-*d*₆, 500 MHz) δ: 7.32–7.39 (m, 6H), 7.42–7.46 (m, 4H), 7.48 (bs, 4H), 7.82 (d, *J* = 8.78 Hz, 1H), 8.06 (d, *J* = 8.78 Hz, 1H), 8.35 (s, 1H), 9.07 (s, 1H), 9.35 (s, 1H). ¹³C NMR (DMSO-*d*₆, 125 MHz) δ: 113.9, 114.4, 120.9, 121.1, 124.4, 128.7, 128.7, 129.2, 129.4, 130.0, 130.3, 130.4, 132.3, 137.5, 139.5, 139.6, 142.0, 142.2, 151.5, 153.0, 153.8. MS Calcd C₂₇H₁₉BrN₄O, 494.1; Found ESI-MS *m/z*: 495.1 (M+1). Retention times, A: 10.4 min and B: 11.1 min.

3.2.4. 1-(4-Bromophenyl)-3-(2,3-di-(pyridin-2-yl)quinoxalin-6-yl)urea **1t**

¹H NMR (DMSO-*d*₆, 500 MHz) δ: 7.32 (m, 2H), 7.49 (bs, 4H), 7.88 (dd, *J* = 8.78 Hz, 1H), 7.91–7.99 (m, 4H), 8.12 (d, *J* = 8.78 Hz, 1H), 8.25 (dd, *J* = 4.88 Hz, *J*₂ = 5.37 Hz, 2H), 8.41 (s, 1H), 9.10 (s, 1H), 9.41 (s, 1H). ¹³C NMR (DMSO-*d*₆, 125 MHz) δ: 113.9, 114.4, 121.1, 123.7, 123.9, 124.4, 124.6, 125.0, 130.1, 132.3, 137.2, 137.4, 137.5, 139.4, 142.0, 142.4, 148.7, 150.8, 153.0, 153.3, 157.8, 157.9. MS Calcd C₂₅H₁₇BrN₆O, 496.1; Found ESI-MS *m/z*: 497.1 (M+1). Retention times, A: 7.1 min and B: 8.5 min.

3.2.5. 1-(3-Bromophenyl)-3-(2,3-di-(furan-2-yl)quinoxalin-6-yl)urea **1u**

¹H NMR (DMSO-*d*₆, 500 MHz) δ: 6.66–6.70 (m, 4H), 7.19 (d, *J* = 7.81 Hz, 1H), 7.27 (t, *J* = 7.81 Hz, 1H), 7.38 (d, *J* = 8.78 Hz, 1H), 7.82 (dd, *J* = 2.44 Hz, *J*₂ = 8.78 Hz, 1H), 7.83–7.88 (m, 3H), 8.01 (d, *J* = 8.78 Hz, 1H), 8.30 (d, *J* = 2.44 Hz, 1H) 9.16 (s, 1H), 9.43 (s, 1H). ¹³C NMR (DMSO-*d*₆, 125 MHz) δ: 112.6, 112.7, 112.8, 113.4, 113.8, 118.0, 121.4, 122.4, 124.9, 125.5, 129.5, 129.9, 131.5, 136.9, 140.06, 141.7, 141.8, 142.3, 143.0, 145.1, 145.5, 151.2, 151.3, 152.9. MS Calcd C₂₃H₁₅BrN₄O₃, 474.0; Found ESI-MS *m/z*: 475.0 (M+1). Retention times, A: 9.2 min and B: 10.1 min.

3.2.6. 1-(2-Bromophenyl)-3-(2,3-di-(furan-2-yl)quinoxalin-6-yl)urea **1v**

¹H NMR (DMSO-*d*₆, 500 MHz) δ: 6.66–6.70 (m, 4H), 7.02 (t, *J* = 7.81 Hz, 1H), 7.39 (t, *J* = 8.3 Hz, 1H), 7.65 (d, *J* = 7.81 Hz, 1H), 7.77 (dd, *J*₁ = 2.44 Hz, *J*₂ = 9.28 Hz, 1H), 7.88 (d, *J* = 9.28 Hz, 2H), 8.03 (d, *J* = 8.78 Hz, 1H), 8.09 (d, *J* = 8.3 Hz, 1H), 8.36 (d, *J* = 2.44 Hz, 1H), 8.38 (s, 1H), 10.05 (s, 1H). ¹³C NMR (DMSO-*d*₆, 125 MHz) δ: 112.7, 112.8, 112.9, 113.5, 113.7, 114.3, 123.4, 124.8, 125.4, 128.9, 130.1, 133.3, 137.0, 137.1, 140.7, 141.8, 142.3, 143.1, 145.2, 145.6, 151.2, 151.3, 152.8. MS Calcd C₂₃H₁₅BrN₄O₃, 474.0; Found ESI-MS *m/z*: 475.1 (M+1). Retention times, A: 9.0 min and B: 10.2 min.

4. Biological activity

4.1. Cell death assays

Doxycycline inducible HeLa cell lines (Dox-GFP, Dox-Noxa, Dox-BadS3A)^{19,20} were induced with doxycycline (Dox = 1 µg/mL) for 3 h. Cells were then treated as indicated for 12 h. Cells were fixed and stained with Hoechst dye and the number of condensed nuclei was counted for each treatment to determine percent cell death.

4.2. Cell growth inhibition assay

Human cervical tumor cells (HeLa) were cultured in RPMI-1640 medium containing 10% FBS and maintained in a 37 °C incubator with 5% CO₂. Cells were plated at 2000 cells/well in 96 well plates and incubated overnight. The next day, cells were treated as indicated. The treated cells were assayed for viability using the alamarBlue assay. Briefly, 10 µL reagent was added to each well and the plate was returned to the incubator for 3 h after which fluorescence at 544_{ex}/590_{em} was measured using a SpectraMax M5e (Molecular Devices) plate reader. The alamarBlue assay was repeated each day for 5 days. Growth is expressed as raw fluorescent units (RFU).

4.3. Caspase 3/7 activation

HeLa cells (2000 cells/well) were treated in 96 well plates as indicated for 6 h. Caspase Glo reagent (Promega, Inc.) was added and luminescence was measured using a SpectraMax M5 (Molecular Devices) plate reader after 1 h. Raw luminescence values (RLU) were normalized to alamarBlue (RFU).

4.4. PARP cleavage

HeLa cells were treated as indicated for 6 h. Cells were harvested by collecting media, trypsinizing cells, and centrifuging to obtain a combined cell pellet from all steps. Cells were lysed in radio immuno precipitation assay (RIPA) buffer (150 mM NaCl, 1.0% Triton X-100, 0.5% sodium deoxycholate, 0.1% sodium dodecyl sulfate, 50 mM Tris, pH 8.0) and protein content was subjected to SDS–PAGE. PARP cleavage was determined via Western blotting using anti-PARP antibody (Calbiochem #AM30).

4.5. Apoptosis protein expression analysis

HeLa cells were treated as indicated for 24 h. Cells were harvested by collecting media, trypsinizing cells, and centrifuging to obtain a combined cell pellet from all steps. Cells were lysed in RIPA buffer and protein content was subjected to SDS–PAGE. Mcl-1 and XIAP expression levels were determined via Western blotting using anti-Mcl-1 antibody (Santa Cruz Biotechnology, Inc. sc-819) and anti-XIAP antibody (Santa Cruz Biotechnology, Inc. sc-58537). Anti-α-tubulin antibody (Cell Signaling Technology, Inc. #3873) was used as a control.

Acknowledgments

This project was supported in part by NIH R01CA127239 and the Eppley Cancer Center pilot Grant. We would like to thank the Eppley NMR facility, Dr. Srikumar Raja for his help with determining CI, Smitha Kizhake for carrying out LC–MS analyses and the Natarajan lab members for helpful discussions.

Supplementary data

Supplementary data associated with this article can be found, in the online version, at doi:10.1016/j.bmc.2012.02.022.

References and notes

- (a) Welsch, M. E.; Snyder, S. A.; Stockwell, B. R. *Curr. Opin. Chem. Biol.* **2010**, *14*, 347–361; (b) Zolova, O. E.; Mady, A. S.; Garneau-Tsodikova, S. *Biopolymers* **2010**, *93*, 777–790; (c) Dawson, S.; Malkinson, J. P.; Paumier, D.; Searcet, M. *Nat. Prod. Rep.* **2007**, *24*, 109–126; (d) Abdelfattah, M. S.; Kazufumi, T.; Ishibashi, M. *J. Nat. Prod.* **2010**, *73*, 1999–2002.
- (a) Greenfield, D. S.; Liebmann, J. M.; Ritch, R. *J. Glaucoma* **1997**, *6*, 250–258; (b) Smith, J. T.; Hamilton-Miller, J. M.; Knox, R. *Nature* **1964**, *203*, 1148–1150; (c) Flore, M. C.; Baker, T. B. *N. Engl. J. Med.* **2011**, *365*, 1222–1231.
- (a) Burke, J. R.; Pattoli, M. A.; Gregor, K. R.; Brassil, P. J.; MacMaster, J. F.; McIntyre, K. W.; Yang, X.; Iotzova, V. S.; Clarke, W.; Strnad, J.; Qiu, Y.; Zusi, F. C. *J. Biol. Chem.* **2003**, *278*, 1450–1456; (b) Baffert, F.; Régner, C. H.; De Pover, A.; Pissot-Soldermann, C.; Tavares, G. A.; Blasco, F.; Brueggen, J.; Chêne, P.; Drucekes, P.; Erdmann, D.; Furet, P.; Gerspacher, M.; Lang, M.; Ledieu, D.; Nolan, L.; Ruetz, S.; Trappe, J.; Vangrevelinghe, E.; Wartmann, M.; Wyder, L.; Hofmann, F.; Radimerski, T. *Mol. Cancer Ther.* **2010**, *9*, 1945–1955.
- Undevia, S. D.; Innocenti, F.; Ramirez, J.; House, L.; Desai, A. A.; Skoog, L. A.; Singh, D. A.; Karrison, T.; Kindler, H. L.; Ratain, M. *J. Eur. J. Biol. Cancer* **2008**, *44*, 1684–1692.
- (a) Johnston, P. A.; Foster, C. A.; Tierno, M. B.; Shun, T. Y.; Shinde, S. N.; Paquette, W. D.; Brummond, K. M.; Wipf, P.; Lazo, J. S. *Assay Drug Dev. Technol.* **2009**, *7*, 250–265; (b) Johnston, P. A.; Soares, K. M.; Shinde, S. N.; Foster, C. A.; Shun, T. Y.; Takyi, H. K.; Wipf, P.; Lazo, J. S. *Assay Drug Dev. Technol.* **2008**, *6*, 505–518.
- Simeonov, A.; Yasgar, A.; Jadhav, A.; Lokesh, G. L.; Klumpp, C.; Michael, S.; Austin, C. P.; Natarajan, A.; Inglesse, J. *Anal. Biochem.* **2008**, *375*, 60–70.
- (a) Cavazzuti, A.; Paglietti, G.; Hunter, W. N.; Gamarro, F.; Piras, S.; Loriga, M.; Allecca, S.; Corona, P.; McIuskey, K.; Tulloch, L.; Gibellini, F.; Ferrari, S.; Costi, M. *Proc. Natl. Acad. Sci. U.S.A.* **2008**, *105*, 1448–1453; (b) Chen, Q.; Bryant, V. C.; Lopez, H.; Kelly, D. L.; Luo, X.; Natarajan, A. *Bioorg. Med. Chem. Lett.* **2011**, *21*, 1929–1932; (c) You, L.; Cho, E. J.; Leavitt, J.; Ma, L. C.; Montelione, G. T.; Anslын, E. V.; Krug, R. M.; Ellington, A.; Robertus, J. D. *Bioorg. Med. Chem. Lett.* **2011**, *21*, 3007–3011; (d) Chen, L. H.; Chang, C. M.; Salunke, D. B.; Sun, C. M. *ACS Comb. Sci.* **2011**, *13*, 391–398.
- Danial, N. N.; Korsmeyer, S. J. *Cell* **2004**, *116*, 205–219.
- Roucou, X.; Montessuit, S.; Antonsson, B.; Martinou, J. C. *Biochem. J.* **2002**, *368*, 915–921.
- Korsmeyer, S. J.; Wei, M. C.; Saito, M.; Weiler, S.; Oh, K. J.; Schlesing, P. H. *Cell Death Differ.* **2000**, *7*, 1166–1173.
- Nuñez, G.; Benedict, M. A.; Hu, Y.; Inohara, N. *Oncogene* **1998**, *17*, 3237–3245.
- Youle, R. J.; Strasser, A. *Nat. Rev. Mol. Cell Biol.* **2008**, *9*, 47–59.
- (a) Awan, F. T.; Kay, N. E.; Davis, M. E.; Wu, W.; Geyer, S. M.; Leung, N.; Jelinek, D. F.; Tschumper, R. C.; Secreto, C. R.; Lin, T. S.; Grever, M. R.; Shanafelt, T. D.; Zent, C. S.; Call, T. G.; Heerema, N. A.; Lozanski, G.; Byrd, J. C.; Lucas, D. M. *Blood* **2009**, *113*, 535–537; (b) Fennell, D. A. *Clin. Lung Cancer* **2003**, *4*, 307–313; (c) Kausch, I.; Jiang, H.; Thode, B.; Doehn, C.; Krüger, S.; Jocham, D. *Eur. Urol.* **2005**, *47*, 703–709.
- Muchmore, S. W.; Sattler, M.; Liang, H.; Meadows, R. P.; Harlan, J. E.; Yoon, S. H.; Nettesheim, D.; Chang, B. S.; Thompson, C. B.; Wong, S. L.; Ng, S. L.; Fesik, S. W. *Nature* **1996**, *381*, 335–341.
- (a) Petros, A. M.; Dinges, J.; Augeri, D. J.; Baumeister, S. A.; Betebenner, D. A.; Bures, M. G.; Elmore, S. W.; Hajduk, P. J.; Joseph, M. K.; Landis, S. K.; Nettesheim, D. G.; Rosenberg, S. H.; Shen, W.; Thomas, S.; Wang, X.; Zanze, I.; Zhang, H.; Fesik, S. W. *J. Med. Chem.* **2006**, *49*, 656–663; (b) Oltersdorf, T.; Elmore, S. W.; Shoemaker, A. R.; Armstrong, R. C.; Augeri, D. J.; Belli, B. A.; Bruncko, M.; Deckwerth, T. L.; Dinges, J.; Hajduk, P. J.; Joesph, M. K.; Kitada, S.; Korsmeyer, S. J.; Kunzer, A. R.; Letai, A.; Li, C.; Mitten, M. J.; Nettesheim, D. G.; Ng, S.; Nimmer, P. M.; O'Connor, J. M.; Oleksijew, A.; Petros, A. M.; Reed, J. C.; Shen, W.; Tahir, S. K.; Thompson, C. B.; Tomaselli, K. J.; Wang, B.; Wendt, M. D.; Zhang, H.; Fesik, S. W.; Rosenberg, S. H. *Nature* **2005**, *435*, 677–681.
- Van Delft, M. F.; Wei, A. H.; Mason, K. D.; Vandenberg, C. J.; Chen, L.; Czabotar, P. E.; Willis, S. N.; Scott, C. L.; Day, C. L.; Cory, S.; Adams, J. M.; Roberts, A. W.; Huang, D. C. *Cancer Cell* **2006**, *10*, 389–399.
- Tahir, S. K.; Yang, X.; Anderson, M. G.; Morgan-Lappe, S. E.; Sarthy, A. V.; Chen, J.; Warner, R. B.; Ng, S. C.; Fesik, S. W.; Elmore, S. W.; Rosenberg, S. H.; Tse, C. *Cancer Res.* **2007**, *67*, 1176–1183.
- (a) Zheng, L.; Yang, W.; Zhang, C.; Ding, W. J.; Zhu, H.; Lin, N. M.; Wu, H. H.; He, Q. J.; Yang, B. *Cancer Lett.* **2011**, *309*, 27–36; (b) Tromp, J. M.; Geest, C. R.; Breij, E. C.; Elias, J. A.; van Laar, J.; Luijckx, D. M.; Kater, A. P.; Beaumont, T.; Van Oers, M. H.; Eldering, E. *Clin. Cancer Res.* **2011**, *18*, 487–489.
- Zhang, L.; Lopez, H.; George, N. M.; Liu, X.; Pang, X.; Luo, X. *Cell Death Differ.* **2011**, *18*, 864–873.
- Lopez, H.; Zhang, L.; George, N. M.; Liu, X.; Pang, X.; Evans, J. J.; Targy, N. M.; Luo, X. *J. Biol. Chem.* **2010**, *285*, 15016–15026.
- (a) Azmi, A. S.; Wang, Z.; Philip, P. A.; Mohammad, R. M.; Sarkar, F. H. *Expert Opin. Emerg. Drugs* **2011**, *16*, 59–70; (b) Dai, Y.; Grant, S. *Cancer Res.* **2007**, *67*, 2908–2911.
- Thomas, L. W.; Lam, C.; Edwards, S. W. *FEBS Lett.* **2010**, *584*, 2981–2989.
- (a) Grande, F.; Aiello, F.; De Grazia, O. D.; Brizzi, A.; Garofalo, A.; Neamati, N. *Bioorg. Med. Chem.* **2007**, *15*, 288–294; (b) Gavara, L.; Saugues, E.; Alves, G.; Debiton, E.; Anizon, F.; Moreau, P. *Eur. J. Med. Chem.* **2010**, *55*, 520–526.
- Bryant, V. C.; Kishore Kumar, G. D.; Nyong, A. M.; Natarajan, A. *Bioorg. Med. Chem. Lett.* **2012**, *22*, 245–248.
- (a) Murata, T.; Shimada, M.; Sakakibara, S.; Yoshino, T.; Masuda, T.; Shintani, T.; Sato, H.; Koriyama, Y.; Fukushima, K.; Nunami, N.; Yamauchi, M.; Fuchikami,

- K.; Komura, H.; Watanabe, A.; Ziegelbauer, K. B.; Bacon, K. B.; Lowinger, T. B. *Bioorg. Med. Chem. Lett.* **2004**, *14*, 4019–4022; (b) Sanda, T.; Lida, S.; Ogura, H.; Asamitsu, K.; Murata, T.; Bacon, K. B.; Ueda, R.; Okamoto, T. *Clin. Cancer Res.* **2005**, *11*, 1974–1982; (c) Okumura, K.; Huang, S.; Sinicrope, F. A. *Clin. Cancer Res.* **2008**, *14*, 8132–8142.
26. (a) Chou, T. C. *Pharmacol. Rev.* **2006**, *58*, 621–681; (b) Chou, T. C. *Cancer Res.* **2010**, *70*, 440–446; (c) Raja, S. M.; Clubb, R. J.; Ortega-Cava, C.; Williams, S. H.; Bailey, T. A.; Duan, L.; Zhao, X.; Reddi, A. L.; Nyong, A. M.; Natarajan, A.; Band, V.; Band, H. *Cancer Biol. Ther.* **2011**, *11*, 263–276.
27. Shi, Y. *Mol. Cell* **2002**, *9*, 459–470.
28. Durlez, P. J.; Shah, G. M. *Biochem. Cell Biol.* **1997**, *75*, 337–349.
29. (a) Dubrez-Daloz, L.; Dupoux, A.; Cartier, J. *Cell Cycle* **2008**, *7*, 1036–1046; (b) Riedl, S. J.; Renatus, M.; Schwarzenbacher, R.; Zhou, Q.; Sun, C.; Fesik, S. W.; Liddington, R. C.; Salvesen, G. S. *Cell* **2001**, *104*, 791–800.
30. Chai, J.; Shiozaki, E.; Srinivasula, S. M.; Wu, Q.; Datta, P.; Alnemri, E. S.; Shi, Y. *Cell* **2001**, *104*, 769–780.